doi:10.1093/jmcb/mjz053
Published online June 25, 2019

Article

Hyperandrogenism in POMCa-deficient zebrafish enhances somatic growth without increasing adiposity

Chuang Shi[1,2], Yao Lu[1,2], Gang Zhai[1], Jianfei Huang[1,2], Guohui Shang[1,2], Qiyong Lou[1], Dongliang Li[3], Xia Jin[1], Jiangyan He[1], Zhenyu Du[3], Jianfang Gui[1], and Zhan Yin[1,4,*]

[1] State Key Laboratory of Freshwater Ecology and Biotechnology, Institute of Hydrobiology, Chinese Academy of Sciences, Wuhan 430072, China
[2] University of Chinese Academy of Sciences, Beijing 100049, China
[3] School of Life Sciences, East China Normal University, Shanghai 200241, China
[4] The Innovative Academy of Seed Design, Chinese Academy of Sciences, Beijing 100864, China
* Correspondence to: Zhan Yin, E-mail: zyin@ihb.ac.cn

Edited by Anming Meng

The endocrine regulatory roles of the hypothalamic–pituitary–adrenocortical axis on anxiety-like behavior and metabolic status have been found throughout animal taxa. However, the precise effects of the balancing adrenal corticosteroid biosynthesis under the influence of adrenocorticotrophic hormone (ACTH), a pro-opiomelanocortin (POMC)-derived peptide, on animal energy expenditure and somatic growth remain unknown. POMC has also been identified as one of the candidate loci for polycystic ovary syndrome, which features hyperandrogenism and some prevalence of obesity in patients. Here we show that zebrafish lacking functional POMCa exhibit similar phenotypes of stress response and body weight gain but not obesity as observed in mammalian models. In contrast with the impaired anorexigenic signaling cascade of melanocyte-stimulating hormones and leptin, which are responsible for their obesity-prone weight gain observed in various *pomc* mutant mammals, analyses with our *pomca* mutant series indicate that ACTH is the key regulator for the phenotype with enhanced somatic growth without obesity in *pomca*-deficient zebrafish. Hypocortisolism associated with hyperandrogenism has been observed in the *pomca*-deficient zebrafish, with enhanced activation of mammalian target of rapamycin complex 1; reutilization of amino acids and fatty acid β-oxidation are observed in the muscle tissue of the *pomca*-deficient fish. After reducing hyperandrogenism by crossing our *pomca* mutant fish with a *cyp17a1*-deficient background, the phenotype of enhanced somatic growth in *pomca*-deficient fish was no longer observed. Thus, our work also demonstrated that the role of POMCa in stress response seems to be conserved in vertebrates, whereas its effect on adipostasis is unique to teleosts.

Keywords: anabolic metabolism, HPI axis, *pomca*, somatic growth, stress response

Introduction

Stress has been defined as a state of irregular homeostasis that results in many physiological, behavioral, and metabolic changes. The hypothalamic–pituitary–adrenal (HPA) invertebrates or hypothalamic–pituitary–interrenal (HPI) axis in teleosts regulates essential physiological adaptations to stress through the secretion of corticosteroids and catecholamines. One key pituitary regulator is the pro-opiomelanocortin (POMC) precursor peptide, which is processed by tissue-specific proteolysis into a series of biologically active components including α-melanocyte-stimulating hormone (α-MSH), adrenocorticotrophic hormone (ACTH), β-MSH, and β-endorphin (β-END) (Gonzalez–Nunez et al., 2003). The effects of mammalian POMC on pigmentation abnormalities, obesity, and adrenal insufficiency have been revealed in many previous analyses of *pomc*-deficient mice models and human patients (Krude et al., 1998; Yaswen et al., 1999; Martin et al., 2011). On the other hand, an association between various polymorphisms of *pomc* and polycystic ovary syndrome (PCOS), which shows hyperandrogenism as

Received January 3, 2019. Revised March 17, 2019. Accepted May 17, 2019.

its key feature, has been observed (Urbanek et al., 1999; Ewens et al., 2010; Pau et al., 2013). However, the pathogenesis of these *pomc* polymorphisms in PCOS, especially related to hyperandrogenism, has never been characterized. Additionally, associations of body weight gain and obesity in the absence of β-MSH and β-END in humans, mice, Labrador retrievers, and flat-coat retrievers have been reported (Rubinstein et al., 1996; Lee et al., 2006; Raffan et al., 2016), indicating that the selection of genomic variants of POMC signaling might also be involved in animal domestication. In addition, many PCOS patients exhibit some degree of insulin resistance and obesity as well (Dunaif et al., 1989).

The HPI axis in fish is largely conserved across vertebrates (Alsop et al., 2009). Compared with mammalian POMC, zebrafish POMCa contains highly conserved regions similar to α-MSH, ACTH, β-MSH, β-END, and possible N-POMC-derived peptides but lacks γ-MSH. However, two *pomc* genes, *pomca* and *pomcb*, have been identified in zebrafish (Gonzalez-Nunez et al., 2003). Only *pomca* appears to be expressed in the pituitary gland and is responsible for the interrenal organ development in zebrafish (Hansen et al., 2003; To et al., 2007). In zebrafish, knockdown of POMCa via injection of a designed antisense morpholino oligonucleotide resulted in a significant reduction of ACTH immunoreactivity and attenuated melanosome dispersal at 5 days postfertilization (dpf) (Wagle et al., 2011). With no available reported teleost *pomc*-specific mutant, no further *in vivo* functional studies have been conducted on the roles of POMC in the regulation of homeostasis and behaviors in adult zebrafish.

To understand the behavioral and metabolic functions of POMC and exploit the functional evolutionary course of POMC in vertebrates and the potential strategies for the genetic selection of farmed fish in aquaculture, a series of mutant lines of *pomca*-deficient zebrafish, a cyprinid model fish, were generated with a transcription activator-like effector nucleases (TALENs) approach. Utilizing our series of *pomca* mutants, we determined that enhanced somatic growth is associated with decreased levels of both anxiety-like behaviors and minimal oxygen consumption rates but not significantly associated with the phenotypic changes in appetite and pigmentation. Under normal feeding conditions, zebrafish without β-MSH and β-END exhibited no obvious abnormalities, and the rest of our *pomca* mutant lines exhibited enhanced somatic growth in contrast to the obesity observed in all *pomc*-null mammals. Regarding the alerted adrenal corticosteroid biosynthesis in the *pomca* mutant fish, hypocortisolism and hyperandrogenism have been observed. *Cyp17a* encodes the enzyme that controls the rate-limiting steps in androgen biosynthesis. Utilizing the *cyp17a1*-deficient fish model generated in our laboratory (Zhai et al., 2017), a *pomca*-/*cyp17a1*-deficient double mutant was produced. No significant enhanced somatic growth, together with increased body lipid contents, has been observed in these *pomca*/*cyp17a1* double mutants. This clearly indicates the essential role of hyperandrogenism in enhanced somatic growth without obesity observed in *pomca* mutant fish. Our findings reveal divergent energy homeostasis under the influence of POMC signaling in teleosts from that in mammals. This also suggests that the genetic markers associated with impaired POMC signaling could be potentially utilized for genetic selection to improve the domestication-related traits of farmed fish growth.

Results

POMCa deficiency disrupted dark-induced melanosome dispersal in larval zebrafish

To investigate the physiological role of *pomca*, the TALENs technique was used to disrupt functional POMCa in zebrafish (Figure 1A). Two independent *pomca* mutant 1 lines (M1), mutant 1 line 1 (M1L1) and mutant 1 line 2 (M1L2), were generated with an 8-bp deletion and 8-bp insertion, respectively. The mutations resulted in premature stop codons that produced truncated proteins of 51 amino acids (aa) and 89 aa for M1L1 and M1L2, respectively (Figure 1B), which caused the deficiency of all the hormones derived from POMCa according to Supplementary Figure S1A. In M1 fish, knockout of the POMCa was evident by a notable reduction in the α-MSH immunoreactivity in the pituitary gland at the adult stage (Figure 1C). The mutation of *pomca* enhanced GFP expression patterns in pituitary gland of *pomca*: GFP-transgenic zebrafish. Furthermore, a significantly decreased expression pattern of *pomca* was observed in M1 zebrafish pituitary gland and hypothalamic at 3 dpf (Figure 1D). The *pomca* mRNA expression in M1 zebrafish decreased significantly at 3 dpf (Figure 1E). These results indicated that *pomca* mRNA is voluntarily degraded in M1 zebrafish. The plasma levels of cyclic AMP (cAMP), reflecting downstream effects of melanocortin receptors, decreased significantly with a reduction of 33% in M1 zebrafish (Table 1).

To evaluate food intake at the larval stage, lipophilic tracer 4-Di-10-ASP-labeled paramecia were used. No obvious differences between M1 zebrafish and wild-type (WT) controls were observed in terms of food intake at 6 dpf (Figure 1F and G). However, M1 zebrafish exhibited hyperphagia at 5 months postfertilization (mpf), when food intake increased by 52% compared to WT siblings (Figure 1H).

Background adaptation is the process of changing color to blend with the hue of the local environment and is also a typical stress response. This process is mediated by MSH via promoting melanosome dispersal. As seen in *pomca*-morphants (Wagle et al., 2011), attenuated melanosome dispersal in darkness (Figure 1I) and a 47.54% decrease of the melanosome area in the M1 zebrafish were observed (Figure 1J).

Disruption of POMCa reduced anxiety-like behavioral responses and oxygen consumption in zebrafish

Significantly reduced expression levels of hydroxyl-delta-5-steroid dehydrogenase-3β- and steroid delta-isomerase 1 (*hsd3β1*), a key enzyme for cortisol synthesis, in M1 zebrafish interrenal gland were observed at 3 dpf (Figure 2A). Accordingly, a significant decrease in cortisol levels was observed in both M1 larval and adult zebrafish plasma, with reductions of

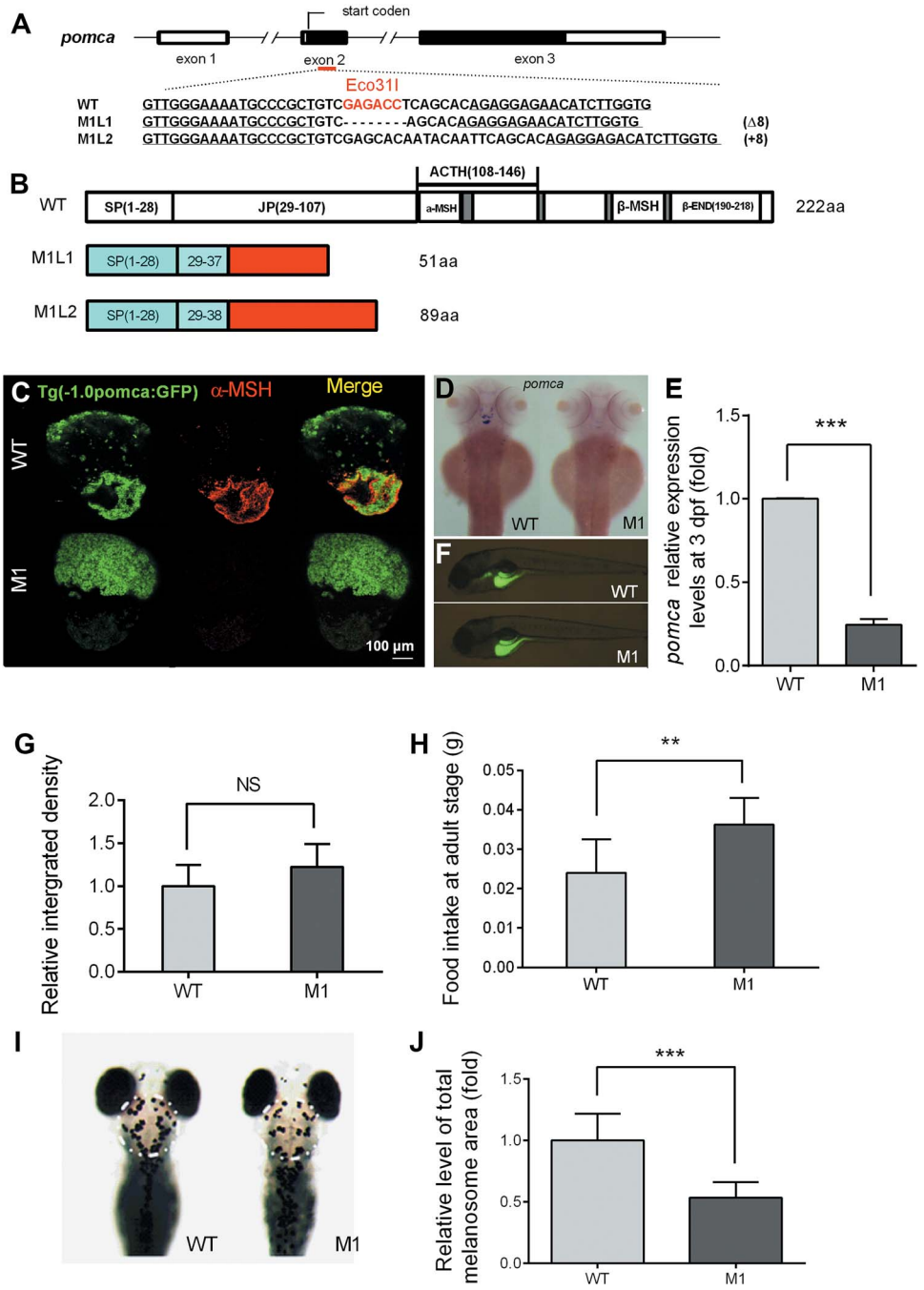

Figure 1 Disruption of *pomca* caused impaired dark-induced melanosome dispersal in larval zebrafish. (**A**) The schematic represents engineered TALENs on *pomca*, exon 2. The underlined fonts indicate the sequences of the two targeting arms of TALENs, and the red fonts show the cutting site of restriction enzyme Eco31I. (**B**) The diagram shows the predicated POMCa protein from WT, M1L1, and M1L2 zebrafish. The mutant lines with putative peptides identical to those of WT fish are shown as blue areas, and the red areas indicate miscoded amino acids. (**C**) GFP (*pomca*: GFP) expression pattern and α-MSH immunofluorescence of the pituitary gland in *pomca* M1 fish and WT control siblings at 150 dpf. (**D**) Dorsal view of endogenous *pomca* mRNA expression patterns in the pituitary gland and hypothalamic of WT ($n = 12$) and *pomca* M1 fish ($n = 10$) at 3 dpf. (**E**) Relative expression levels of *pomca* mRNA in *pomca* M1 fish and WT zebrafish at 3 dpf ($n = 3$/group). (**F**) Feeding assay of WT and *pomca* M1 zebrafish using 4-Di-10-ASP-labeled paramecia at 6 dpf. (**G**) Relative levels of ingested paramecia shown as fluorescence intensities ($n = 7$/group). (**H**) Total food intake in 2 h by WT and *pomca* M1 adult fish after 5 days of starvation ($n = 8$–10/group). (**I**) Image of 4 dpf WT and *pomca* M1 fish exposed to darkness for 30 min. The area of melanosome measurement is shown by the white circle. (**J**) The diagram shows the relative values of total melanosome area of the indicated regions ($n = 10$/group). 'NS' indicates that there were no significant differences between two groups.

Table 1 cAMP, cortisol, and testosterone concentrations.

Test	Sample	Wild-type siblings	*pomca* M1 fish
cAMP	Plasma (pmol/ml)	56.0 ± 11.31	37.0 ± 5.70*
Cortisol	Whole larvae fish(pg/larvae)	14.89 ± 2.57	3.63 ± 0.84***
	Plasma (pg/μl)	151.6 ± 38.03	22.24 ± 6.66**
Testosterone	Plasma (pg/μl)	5.40 ± 2.35	13.81 ± 2.31**

Data are represented as mean ± SD. *$P \leq 0.05$, **$P \leq 0.01$, ***$P \leq 0.001$ (Student's *t*-test).

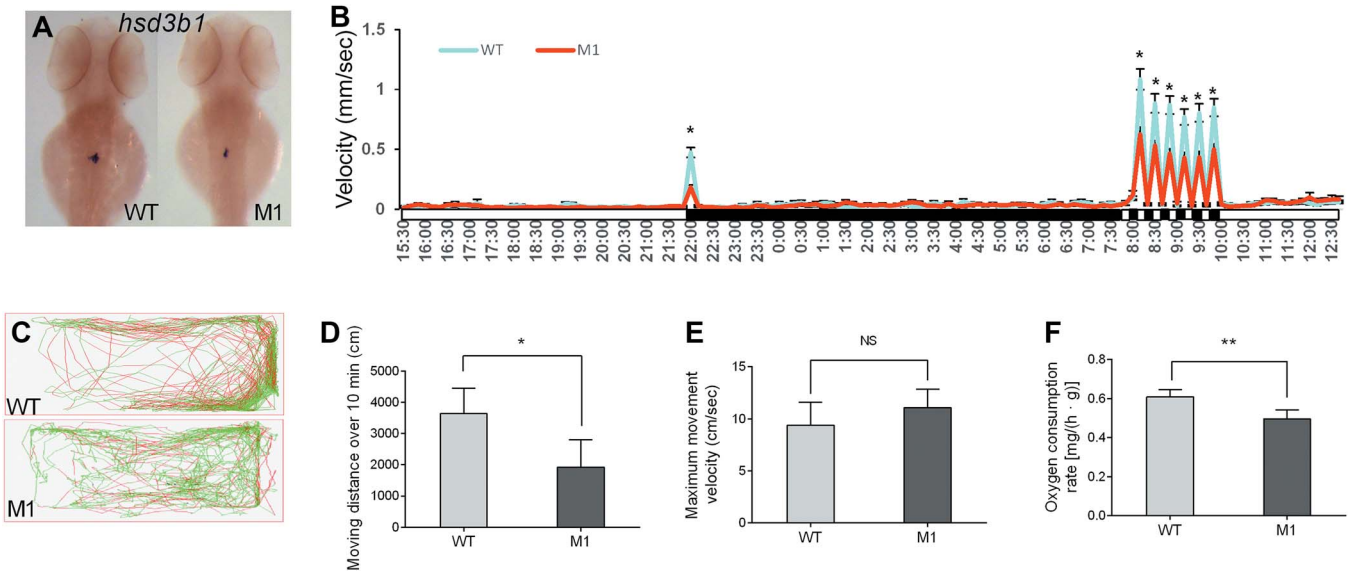

Figure 2 POMCa deficiency reduced anxiety-like behaviors and basal metabolism in zebrafish. (**A**) Whole-mount *in situ* hybridization (WISH) assay of *hsd3b1* expression in interrenal glands of WT ($n = 10$) and *pomca* M1 fish ($n = 10$) at 3 dpf. (**B**) The dark–light emergence test was applied to larval zebrafish at 4 dpf. The white boxes below the horizontal line indicate periods of light, and the black boxes represent periods of darkness ($n = 48$/group). (**C**) The locomotor trajectory of WT and *pomca* M1 adult fish within 10 min. The movement velocity >8 cm/sec and <1 cm/sec are represented by red and gray locomotor trajectories, respectively. The movement velocity between 1 and 8 cm/sec is represented by a green locomotor trajectory. (**D**) Total distance moved over 10 min by WT and *pomca* M1 fish ($n = 6$/group). (**E**) The maximum movement velocity within 10 min ($n = 6$/group). (**F**) The oxygen consumption rates of WT and *pomca* M1 fish were measured at 150 dpf after 5 days of starvation ($n = 4$/group). 'NS' indicates that there were no significant differences between two groups.

75.59% and 85.33%, respectively (Table 1). The dark–light emergence test performed on 4 dpf larval zebrafish was used to examine anxiety-related behavioral responses (Peng et al., 2016). The reduced locomotor activity of *pomca* M1 fish in response to illumination transitions was recorded (Figure 2B). Moreover, analyses of adult zebrafish movement behavior and swimming trajectory also indicated that the distance moved by M1 zebrafish decreased significantly with a reduction of 46.14% compared with control siblings (Figure 2C and D) but with similar peak velocities (Figure 2E), suggesting that the recorded difference of behavior was not due to a defect in muscle capacity.

The metabolic rate of fish is ordinarily reflected by their oxygen consumption rate (Rosa et al., 2008). M1 zebrafish exhibited significantly lower oxygen consumption rates, with a reduction of 18.39% compared with control zebrafish (Figure 2F), a phenomenon that was also previously reported in *pomc*-deficient mice (Coll et al., 2005).

Disruption of pomca promoted somatic growth, but not adiposity, in adult zebrafish

Raised in the same tank to compare somatic growth and related features, the body weights and body lengths of M1 fish and WT fish were examined periodically every month after the onset of feeding. No obvious difference was observed in somatic growth prior to their juvenile stages. However, at 65 dpf stage, M1 zebrafish began to exhibit greater body weights and lengths than their WT siblings (Figure 3A–C). The increased rates of the M1 zebrafish compared with those of the WT zebrafish were 18.01% for body weight and 5.75% for body length at 65 dpf. Deletion of POMC caused severe early-onset obesity in mice (Coll et al., 2005). However, lipid content was not significantly different between M1 fish and their WT siblings when both groups were raised in the same tank using a normal feeding protocol. Moreover, in the overfeeding paradigm, although the *pomca* M1 fish showed a much greater body weights and body lengths (Figure 3D and E), the total lipid content of the two *pomca*

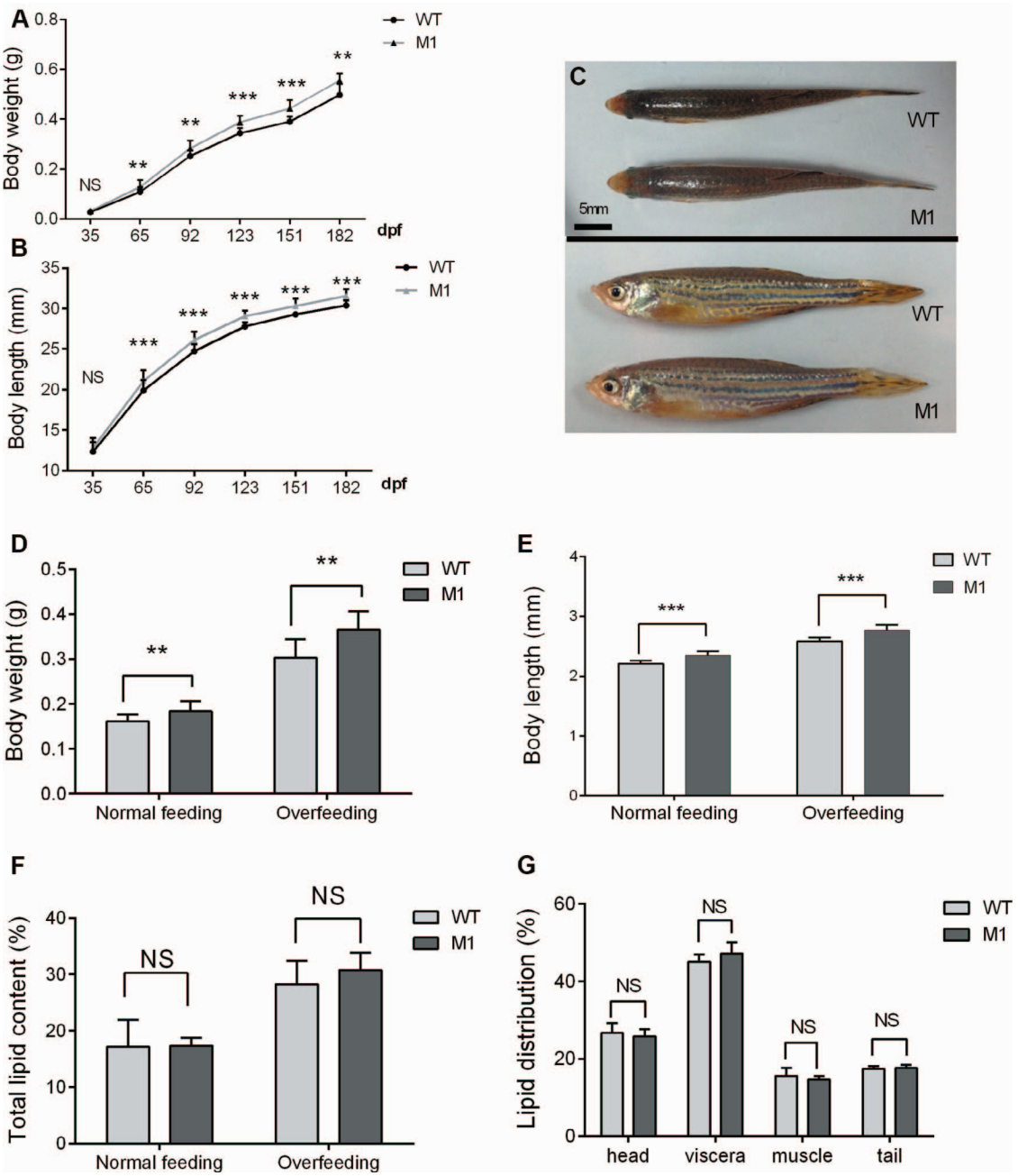

Figure 3 Disruption of POMCa enhanced somatic growth without lipid content changes in zebrafish. (**A** and **B**) Curves of body weight (**A**) and body length (**B**) of zebrafish from the juvenile stage to the adult stage (n = 20–30/group). (**C**) Dorsal view and lateral view of WT and *pomca* M1 fish at 90 dpf stage. (**D**–**F**) Body weight (**D**), body length (**E**), and total lipid content (**F**) of *pomca* M1 fish and WT control siblings under normal feeding and overfeeding protocols (n = 6–10/group). (**G**) The lipid distribution of *pomca* M1 fish and WT control siblings in the head, viscera, muscle, and tail tissues (n = 4–5/group). 'NS' indicates that there were no significant differences between two groups.

genotypic groups were not different (Figure 3F). In addition, no significant difference was observed in lipid distribution in head, viscera, muscle, or tail tissue between M1 fish and WT controls (Figure 3G).

Pomc-null mice exhibited higher fed blood glucose levels and plasma insulin levels than their WT sibling littermates (Coll et al., 2005). Interestingly, no significant difference in blood glucose levels in adult M1 fish and WT controls was observed at 30 min postfeeding (Supplementary Figure S2A). Moreover, the mRNA expression levels of *insulin a* (*insa*), *glucagon a* (*gcga*), and *leptin a* (*lepa*) genes were not altered in M1 zebrafish at 4 dpf or at the adult stage compared with WT controls (Supplementary Figure S2B and C). We also crossed our *pomca* M1 fish with the transgenic reporter zebrafish line carrying a β-cell marker

[Tg (−1.2 *insulin*: GFP)]. The morphology and size of pancreatic β-cells between M1 fish and the control fish were not different at 5 dpf (Supplementary Figure S2D and E). Although pituitary gland size was changed in M1 fish, no differences in M1 fish and the WT fish regarding the expression patterns of pituitary hormone genes (except *pomca*) were found. Moreover, the key factors involved in growth hormone signaling were also unchanged in M1 fish hepatic tissue (Supplementary Figure S3A–C).

Deletion of pomca enhanced protein synthesis and fatty acid β-oxidation in muscle tissue

The histological examinations through sectioning and hematoxylin and eosin (H&E) staining indicated that the total muscle area in M1 zebrafish increased significantly and showed more muscle fibers compared with WT siblings (Figure 4A–D), suggesting that excessive muscle growth was due to myocyte hyperplasia. The expression level of the phospho-s6 ribosomal protein (p-S6), a substrate of mammalian target of rapamycin complex 1 (mTORC1) in muscle tissue of the M1 zebrafish increased significantly in comparison with control siblings (Figure 4E and F). Additionally, elevated phosphorylated AKT levels were observed in muscle tissue of M1 zebrafish compared with those of control fish. The increased body weight in M1 zebrafish was reversed after the treatment of two independent mTORC1 inhibitors, rapamycin and AZD8055 (Figure 4G). Thus, these observations suggest enhanced activation of the mTORC1 pathway in M1 fish muscle tissue.

To further confirm the role of POMCa in the regulation of protein synthesis and fatty acid β-oxidation, we measured [1-^{14}C] palmitate oxidation in muscle tissue homogenates. [1-^{14}C] Palmitate oxidation was increased significantly in M1 fish muscle tissue compared with control fish (Figure 4H). Furthermore, a catabolic rate assay was carried out *in vivo*. Live fish were intraperitoneally injected with an L-[^{14}C(U)] amino acid mixture and D-[1-^{14}C] glucose. The radioactivity in muscle tissue samples was measured. The catabolic rates of amino acids and glucose decreased significantly in M1 zebrafish (Figure 4I). M1 zebrafish showed more retention of the L-[^{14}C(U)] amino acid mixture and D-[1-^{14}C] glucose in muscle tissue than control fish (Figure 4J). These data suggest that *pomca* deficiency promoted fatty acid oxidation and protein synthesis and decreased the catabolic rate of amino acids and glucose in zebrafish muscle tissue.

Deficiency of ACTH–MC2R signaling was a key factor in promoting zebrafish somatic growth

To examine the key players responsible for the phenotypes observed in POMCa-null zebrafish, two additional types of targeted mutations in the zebrafish *pomca* locus were subsequently generated. It has been revealed that the motif (RKRRP, 122–126), which is conserved across all vertebrates and is located between α-MSH and ACTH in the POMC prohormone protein, is critical for the activities of both α-MSH and ACTH (Dores et al., 2014). This motif contains a cleavage region (RKRR, 122–125) and is selectively bound to the ACTH receptor, melanocortin 2 receptor (MC2R). Mutation in this region caused the failure of α-MSH cleavage from the POMCa peptide and caused the impairment of effective interaction between ACTH and MC2R. Therefore, our *pomca* mutant 2 fish (M2) contained a targeted deletion of nine base pairs encoding three critical amino acids (KRR, 123–125) within this crucial conserved region that led to functional disruption of both α-MSH and ACTH but did not affect the processing of β-MSH and β-END at the C-terminal region of the POMCa protein (Figure 5A). Two additional independent mutant lines, mutant 3 line 1 (M3L1) and mutant 3 line 2 (M3L2), were generated with 7-bp and 4-bp insertions at the *pomca* locus, which caused premature stop codons that produced truncated POMCa proteins of 188 aa and 187 aa in M3L1 and M3L2, respectively. These truncated proteins produced proper α-MSH and ACTH peptides but not β-MSH or β-END in *pomca* M3 fish (Figure 5B and C). These additional two *pomca* mutant lines provide ideal models to clarify the precise roles of each POMCa-derived peptide in the function of growth promotion in zebrafish.

After overall phenotypic observations and analyses, we found no difference in *pomca* mRNA expression patterns in M2 and M3 fish compared with control fish at 3 dpf (Figure 5D). M1 and M2 fish exhibited highly similar phenotypes in terms of the features of somatic growth, minimal oxygen consumption, distance moved, and cortisol and testosterone levels, while the only similar phenotype shown in all M1, M2, and M3 lines was a reduced plasma cAMP level (Table 2; Figure 5E and F). Melanocortin peptides regulate pigmentation and appetite by combining with melanocortin 1 receptor (MC1R) and melanocortin 4 receptor (MC4R), respectively (Anderson et al., 2016). All melanocortin peptides have the His-Phe-Arg-Trp (HFRW) motif (Supplementary Figure S1A), which is required for activation of all the MCRs (except MC2R) (Dores et al., 2014). However, M2 fish lacking of α-MSH showed no obvious difference in food intake or melanosome dispersal compared with control siblings (Table 2; Figure 5G). This indicated that increased food intake was not required for somatic growth in *pomca*-deficient zebrafish. Despite the lack of α-MSH and RKRRPs motif, the HFRW motif of ACTH (Δ3aa) in M2 fish was intact. The ACTH (Δ3aa) can still stimulate downstream signaling pathways by binding to MC1R and MC4R. Thus, combined with the data derived from *pomca* M1, M2, and M3 fish, we concluded that the deficiency of ACTH–MC2R signaling is responsible for the phenotypes related to cortisol levels, locomotion patterns, and somatic growth in POMCa-deficient zebrafish.

Mouse genome contains two *pomc* genes, *α-pomc* and *β-pomc*. However, *β-pomc* is regarded as a pseudogene (Notake et al., 1983; Uhler et al., 1983). In zebrafish, *pomcb* is also regarded as a pseudogene (Wagle et al., 2011), which was initially disrupted by using the TALENs technique (Supplementary Figure S4A). A mutant line with an 11-bp deletion was obtained. No significant difference in body weight between *pomcb* mutant fish and WT controls was observed at 3 mpf (Supplementary Figure S4B). Furthermore, depletion of *pomcb* had no effect on

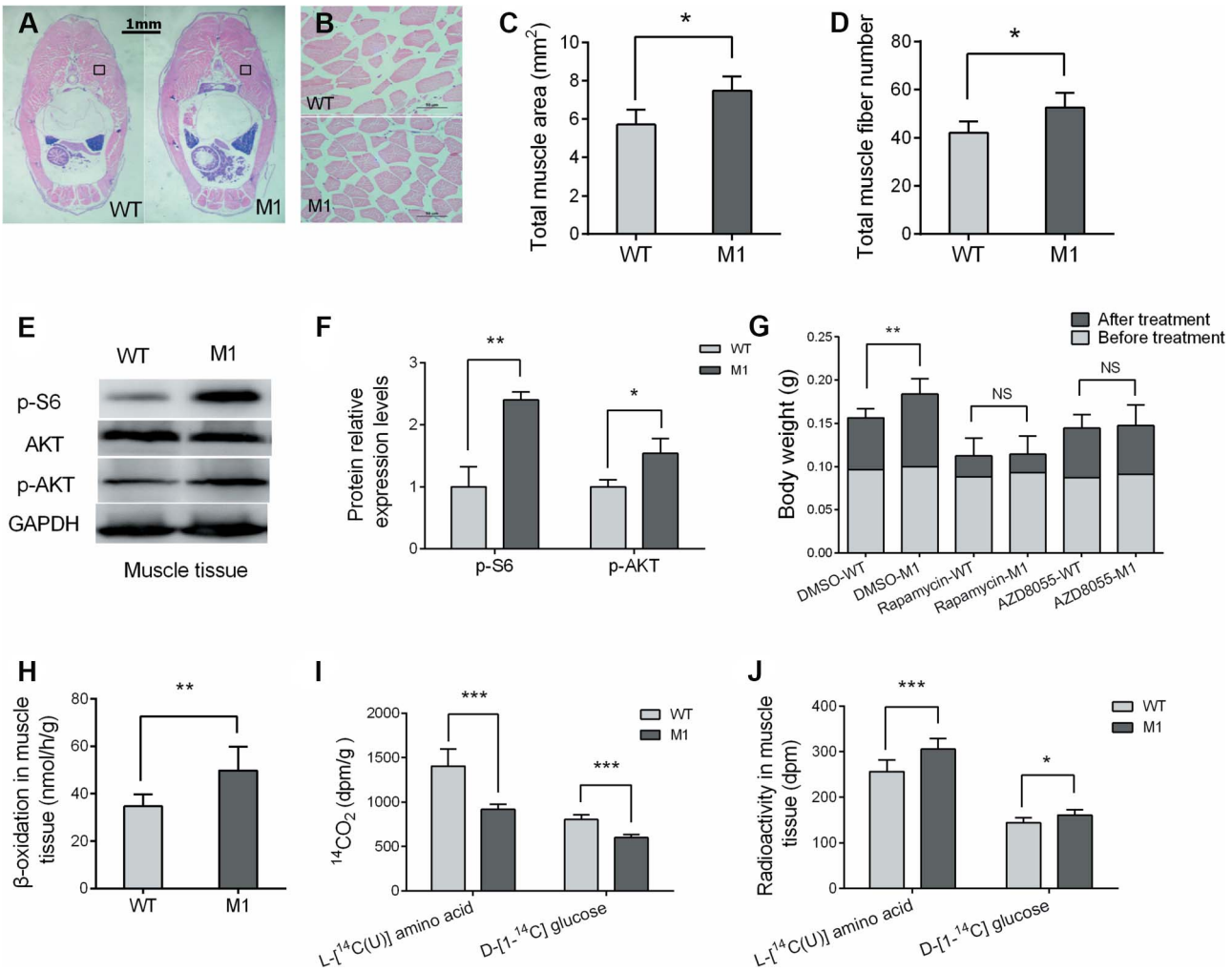

Figure 4 POMCa deficiency increased protein synthesis and fatty acid β-oxidation in muscle tissue. (**A** and **B**) H&E staining of the muscle tissue (**A**) and higher magnification of the indicated regions (**B**). (**C**) The diagram shows the total area of muscle tissue in the body cross-section (n = 5/group). (**D**) The total fiber numbers of the indicated regions of WT and *pomca* M1 fish (n = 5–6/group). (**E**) Western blot analysis of p-s6 and p-AKT proteins from muscle tissue of *pomca* M1 fish and WT fish. GAPDH protein was used as an internal control. (**F**) Western blots were quantified by gray value analysis using ImageJ software (n = 3/group). (**G**) The body weight before and after treatment with two independent mTORC1 inhibitors, rapamycin, and AZD8055 (n = 7–10/group). (**H**) Muscle tissue capacity of mutants and their control siblings to oxidize [1-^{14}C] palmitic acid (n = 6/group). (**I**) The conversion of the intraperitoneally injected L-[^{14}C(U)] amino acid mixture and D-[1-^{14}C] glucose into carbon dioxide in 2 h (n = 6/group). (**J**) Retained radioactivity in muscle after the intraperitoneally injected L-[^{14}C(U)] amino acid mixture and D-[1-^{14}C] glucose (n = 5–6/group). 'NS' indicates that there were no significant differences between two groups.

larval cortisol contents (Supplementary Figure S4C). In addition, no compensative expression pattern of *pomcb* was observed in M1 zebrafish (Supplementary Figure S4D). However, the relative expression of *pomca* in *pomcb* mutant zebrafish was increased compared with control siblings (Supplementary Figure S4E). We crossed *pomca* M1 zebrafish into *pomcb* mutant fish and obtained *pomca/pomcb* double mutant zebrafish. The double mutant fish body weight had no significant difference compared with *pomca* M1 zebrafish at 72 dpf (Supplementary Figure S4F). These data indicate that *pomca* might exhibit certain functions in *pomcb* mutant zebrafish, but *pomcb* has no redundant roles in *pomca* M1 zebrafish.

Essentiality of hypocortisolism and hyperandrogenism for enhanced somatic growth without obesity in POMCa-deficient zebrafish

The plasma levels of testosterone in M1 fish were elevated, with a 1.5-fold increase compared with WT fish (Table 1). In addition, the proportion of males in the M1 group was higher than that in WT control fish at 6-month stage (Supplementary Figure S5A). A series of steroidogenic enzymes such as HSD3β1, CYP17A1, cytochrome P450 family 19 subfamily A polypeptide 1a (CYP19A1a), and 17β-hydroxysteroid dehydrogenase type 3 (HSD17b3) are involved in the steroid biosynthetic pathway, which leads to the synthesis of a variety of steroid

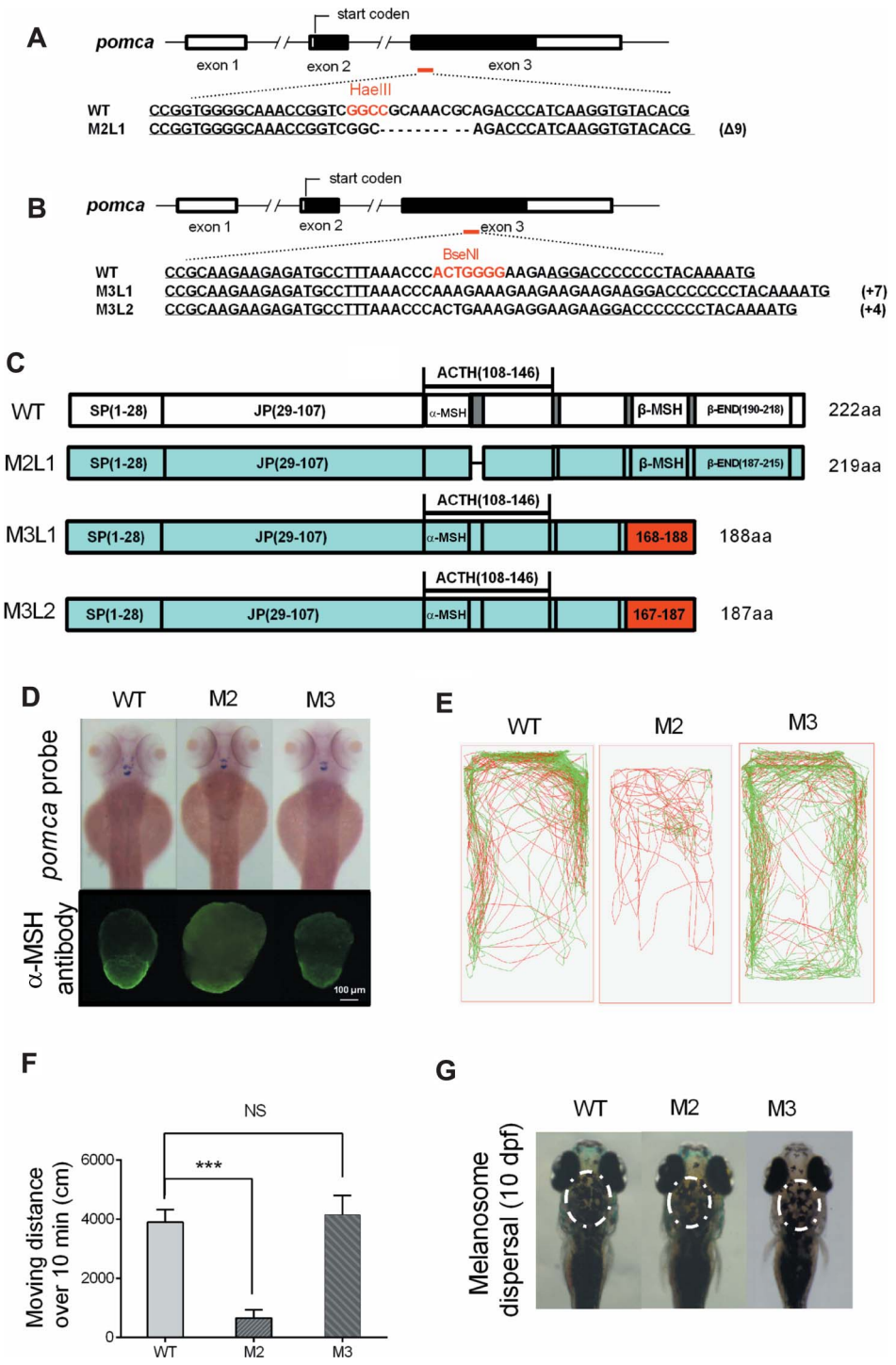

Figure 5 Generation of POMCa truncated mutations in zebrafish via TALENs. (**A**) The schematic represents engineered TALENs in *pomca*. The restriction enzyme HaeIII was used to identify the genotypes. The underlined fonts indicate the sequences of the two targeting arms of TALENs. (**B**) The schematic represents engineered TALENs in *pomca*. Two independent types of *pomca* mutant 3, M3L1 and M3L2, were generated with insertions of 7 bp and 4 bp, respectively. (**C**) The diagrams show the predicated POMCa protein of *pomca* M2 and M3 fish compared with the WT POMCa protein. (**D**) The upper figure shows the dorsal view of endogenous *pomca* mRNA expression in the pituitary gland and hypothalamic of WT ($n = 15$), *pomca* M2 ($n = 13$), and M3 fish ($n = 12$) at 3 dpf. The bottom figure represents α-MSH immunofluorescence of the pituitary gland in *pomca* M2 and M3 fish at 150 dpf. (**E**) The locomotor trajectory of *pomca* M2 and M3 adult fish (bottom) within 10 min. (**F**) Total distance moved of WT, *pomca* M2 and M3 fish over 10 min ($n = 10$/group). (**G**) The melanosome was imaged at 10 dpf following treatment with 30 min darkness. 'NS' indicates that there were no significant differences between two groups.

Table 2 Comparison of the *pomca* mutant lines with wild-type zebrafish.

	WT	M1	M2	M3
α-MSH	√	X	X	√
ACTH	√	X	Δ3aa	√
β-MSH	√	X	√	X
β-END	√	X	√	X
Body weight (g)	0.252 ± 0.025	0.283 ± 0.032**	0.302 ± 0.041***	0.242 ± 0.026
Body length (mm)	24.72 ± 0.84	26.11 ± 1.05***	26.46 ± 0.94***	24.60 ± 0.84
Plasma testosterone (pg/ul)	5.40 ± 2.35	13.81 ± 2.31**	10.97 ± 1.2*	5.51 ± 1.32
Larvae cortisol (pg/fish)	14.89 ± 2.57	3.63 ± 0.84***	4.17 ± 1.94***	15.46 ± 1.87
Moving distance (cm)	3597.7 ± 404	1937.9 ± 561**	994.4 ± 316.8***	3557.2 ± 196.3
Oxygen consumption	0.608 ± 0.038	0.496 ± 0.04[7]***	0.453 ± 0.083**	0.5523 ± 0.089
Food intake (mg)	23.41 ± 9.14	35.63 ± 7.09**	24.02 ± 7.03	19.69 ± 5.68
cAMP (pmol/ml)	56.0 ± 11.31	37.0 ± 5.70*	43.2 ± 9.87*	28.53 ± 5.74**

X means peptide production is absent in the mutant; √, peptide production present in the mutant; Δ3aa, the ACTH lacking 3 amino acids; data are represented as mean ± SD. $^{*}P \leq 0.05$, $^{**}P \leq 0.01$, $^{***}P \leq 0.001$ (Student's *t*-test).

hormones. The expression levels of the genes involved in cortisol and testosterone biosynthesis in the head kidney (where fish interrenal tissue is located) were examined by quantitative real-time PCR (qRT-PCR) (Figure 6A). Similar to the WISH analysis results shown in Figure 2A, the expression levels of *hsd3b1* decreased by ∼60% in *pomca* M1 fish head kidney tissue samples compared with those in control samples, whereas the mRNA level of *hsd17b3*, which encodes the enzyme for the final conversion of androstenedione into testosterone, was upregulated 2.8-fold in M1 fish (Figure 6A). The genes involved in cortisol and testosterone biosynthesis were also examined in the testis. However, there were no differences in the expression patterns of these genes between M1 fish and WT control fish except for *cyp19a1a* and *hsd17b3* (Supplementary Figure S5B). These data indicated that elevated plasma testosterone was synthesized in the interrenal gland but not the testis.

To verify the role of hyperandrogenism in the phenotypes of enhanced somatic growth and fatty acid oxidation observed in M1 fish, we crossed our M1 fish with *cyp17a1* mutant fish in which testosterone levels were significantly decreased (Zhai et al., 2017). Intriguingly, the *pomca* and *cyp17a1* double mutant fish (M1/*cyp17a1*$^{-/-}$) showed no significant difference in terms of body weight compared with that of WT sibling fish at 3-month stage (Figure 6B). The oxygen consumption rate was decreased in M1/*cyp17a1*$^{-/-}$ fish compared with WT fish (Figure 6C). Moreover, the M1/*cyp17a1*$^{-/-}$ fish displayed significantly higher lipid contents compared to WT and *pomca* M1 fish (Figure 6D). These data suggest that depletion of *pomca* can lead to hyperandrogenism, which is necessary for enhanced somatic growth without obesity in our *pomca* mutant fish.

Discussion

Utilizing TALENs approach, a series of *pomca* mutant lines of zebrafish were generated. Transcription levels of *pomca* and of the existing of α-MSH epitope in the pituitary gland were assessed in *pomca* mutant fish (Figures 1C–E and 5D). Quantification of melanosome dispersal and locomotion activity of zebrafish in response to the dark–light transition was performed for assessment of camouflage behavior and startle response, representing the stress responses involved in MSHs or cortisol regulated by the HPI axis (Wagle et al., 2011; Peng et al., 2016). Impaired melanosome dispersal and reduced swim velocity were observed in M1 zebrafish (Figures 1I, J and 2B–D). Transcriptional expression data of a series of steroidogenic enzymes and the status of the altered adrenal corticosteroid biosynthesis have been evaluated due to the lack of functional ACTH–MC2R signaling in *pomca* mutant lines (Figures 2A and 6A; Tables 1 and 2). Together with the features above, body weight gain and body lipid contents are associated with the weakened capacity of stress responses, decreased minimal oxygen consumption rates, hypocortisolism, and hyperandrogenism but not with alternations of appetite and pigmentation. Most of these associated features may be regulated by ACTH (Gallo-Payet, 2016), suggesting their critical functions in metabolism observed in our *pomca* mutant zebrafish. Most metabolic defects observed in mammalian models have been attributed to the impairments of functional MSH/AgRP/Leptin signaling in various *pomc* mutants reported previously (Coll et al., 2005).

MSHs are known to regulate feeding behavior and camouflage behavior in mammals (Yaswen et al., 1999; Raffan et al., 2016). The α-MSH/β-MSH-mediated suppression of appetite in mammals is attributed to MC4R (Huszar et al., 1997). Increased food intake has also been observed in *mc4r*-deficient zebrafish (Fei et al., 2017). In present study, significant increases in food intake were observed in M1 adult zebrafish (Figure 1H). Since intact and mature β-MSH peptide or α-MSH should be produced in M2 or M3 mutant fish, respectively, no significant increase in food intake was observed in M2 and M3 fish (Table 2). These results confirm the conserved function of α-MSH/β-MSH-mediated suppression of appetite in all vertebrates. However, together with the somatic growth features among these three types of *pomca* mutant fish, our results indicate that increased food intake is not associated with excess body weight gain without obesity.

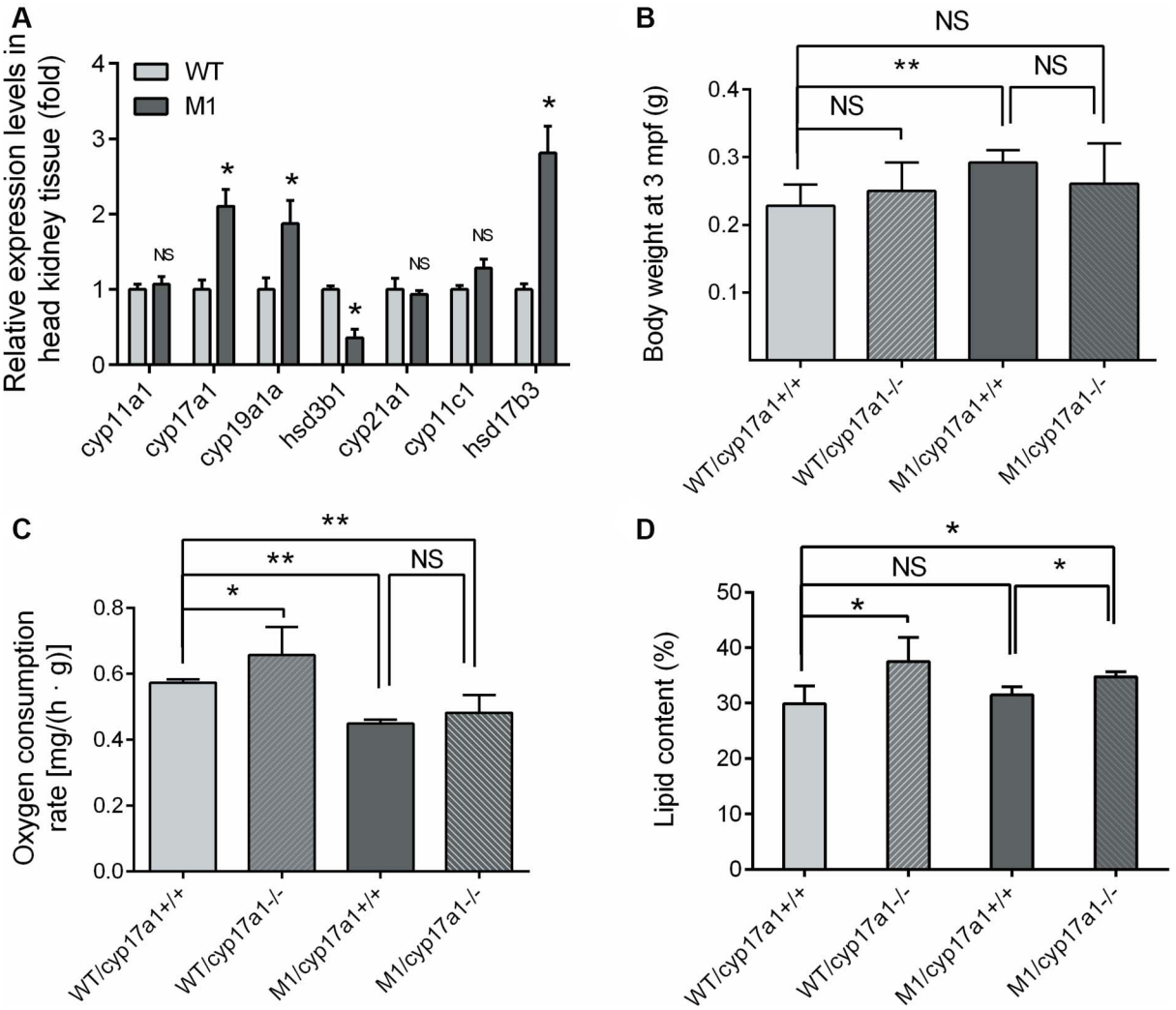

Figure 6 Hypocortisolism and hyperandrogenism are imperative for enhanced somatic growth without obesity in *pomca*-deficient zebrafish. (**A**) The transcriptional levels of key molecules, *cyp11a1*, *cyp17a1*, *cyp19a1a*, *hsd3b1*, *cyp21a1a*, *cyp11c1*, and *hsd17b3*, involved in the cortisol and testosterone synthesis in head kidney tissue ($n = 3$/group) (**B**) The body weight of M1 zebrafish, WT/*cyp17a1* fish, M1/*cyp17a1* fish, and WT control siblings at 3 mpf ($n = 3–4$/group). (**C**) Oxygen consumption rate of the four types of fish at 5 mpf ($n = 3$/group). (**D**) Lipid content of the four fish types at 3 mpf ($n = 3–4$/group). 'NS' indicates that there were no significant differences between two groups.

Interestingly, M1 fish did not exhibit obesity, which has been reported in all *pomc*- and *mc4r*-null mammalian models (Rubinstein et al., 1996; Krude et al., 1998; Yaswen et al., 1999; Raffan et al., 2016). Despite a higher gain in body weight in M1 fish, no significant difference between the body compositions of mutant and control fish under both normal feeding and overfeeding conditions was observed (Figure 3D–F). In mouse models, the expression of *pomc* can be stimulated by the primary adipostatic hormone leptin. The absence of α-MSH in *pomc*-null mice causes obesity, and the blockade of neuronal melanocortin signaling diminishes the response to leptin administered centrally (Schwartz et al., 2000). In contrast to mammalian, fish *leptin* is not significantly expressed in adipose tissue, and its role as an adipostatic factor is likely to be secondary. It might be primarily involved in regulating insulin production and glucose homeostasis (Michel et al., 2016). No obvious body weight and obesity phenotypes have been observed in *mc4r*-deficient and *lepr*-deficient zebrafish using normal feeding protocols (Michel et al., 2016; Fei et al., 2017). The increased food intake, greater body weight, and higher body fat to lean ratio were observed only in *mc4r*-deficient and *lepr*-deficient zebrafish using satiable feeding protocol (Fei et al., 2017). However, another report showed no notable phenotypes related to obesity and food intake in *lepr*-deficient zebrafish using overfeeding paradigm (Michel et al., 2016).

Because of poor conservation of the functional adipostatic hormone leptin, it has been suggested that the functions of the teleost central melanocortin circuits might be related to growth hormone production and signaling (Zhang et al., 2012). However, no significant difference between the expression patterns

of pituitary gland *gh1* or hepatic *igf1* of *pomca* M1 fish and their control fish was detected (Supplementary Figure S3A and C). Notably, several specific mammalian *pomc* mutants missing only β-MSH and β-END also had body weight gain and/or obesity (Rubinstein et al., 1996; Lee et al., 2006; Raffan et al., 2016), whereas similar phenotypes were not observed in M3 fish model with only β-MSH and β-END deficiency, suggesting that increased body weight was associated only with deficiency in α-MSH and/or ACTH in the zebrafish model (Table 2). In the present study, increased body weight without obesity in adult *pomca* M1 and M2 fish were observed under both regular feeding and overfeeding conditions (Figure 3D–F). On the other hand, although higher food intake was observed in the *mc4r*-deficient zebrafish under normal feeding conditions at 3 mpf, no greater body weight gain was observed (Fei et al., 2017). This phenotypic difference in body weight gain between M1 zebrafish and *mc4r*-deficient zebrafish probably resulted from signaling pathways other than those including α-MSH in POMC-null fish *in vivo*. In addition, the enhanced somatic growth observed in M2 fish without increased food intake (Table 2) suggested that some aspects other than appetite regulation could be the primary cause(s) for body weight gain in *pomca* mutant fish.

Fish interrenal tissue is homologous to the adrenal gland in mammals, which is a principal site for the synthesis of steroid hormones, including glucocorticoids, estrogen, and androgens. Among fish interrenal steroidogenic enzymes, HSD3β1 catalyzes and synthesizes δ4 steroids, such as progesterone, the precursor of cortisol, and its expression is associated with the regulation of HPI signaling (Lin et al., 2015). On the other hand, CYP17A1 and CYP19A1 catalyze the formation of estrogen and testosterone, which are critical for adrenal estrogen and androgen production (Tokarz et al., 2013). In humans, HSD3B is essential for adrenal biosynthesis of aldosterone and cortisol. Its expression in the adrenal gland is inversely associated with adrenal estrogen and testosterone levels. HSD3B can influence the production of aldosterone, cortisol, and adrenal androgen by competing with CYP17 for the metabolism of pregnenolone and 17α-hydroxypregnenolone (Rainey and Nakamura, 2008). In fact, we observed the downregulated expression of *hsd3b1* and elevated expression of *cyp17a1a*, *cyp19a1a*, and *hsd17b3* in *pomca* M1 fish head kidney tissue samples compared with control fish (Figure 6A), which echoed with the decreased plasma levels of cortisol and elevated plasma levels of testosterone observed in *pomca* M1 fish (Table 1).

Testosterone can induce energy expenditure in skeletal muscle via enhancing mitochondrial biogenesis and fatty acid β-oxidation (Usui et al., 2014). A significant inverse correlation between total testosterone levels and the degree of obesity has been reported in many studies (Kelly and Jones, 2015). Acting as an anabolic steroid hormone, testosterone also promotes protein synthesis via activating mTORC1 signaling (Rossetti et al., 2017). Usually, testosterone enhanced protein synthesis results in mammalian skeletal muscle growth and hypertrophy (Kadi, 2008). However, excessive muscle growth in teleost skeletal muscle normally manifests as myocyte hyperplasia, not hypertrophy as observed in mammalian models (Li et al., 2014; Gao et al., 2016). Therefore, enhanced body weight gain and skeletal muscle hyperplasia could be derived from the increased level of plasma testosterone in *pomca* M1 fish (Figures 3A–C and 4A–D; Table 1). In effect, enhanced activation of mTORC1 and reutilization of amino acids have been observed in the muscle tissue of *pomca* M1 fish (Figure 4E, F, and J). Elevated fatty acid β-oxidation in M1 fish skeletal muscle samples was also recorded (Figure 4H). To confirm that the elevated testosterone levels mediated these anabolic processes, we generated double mutant zebrafish, which make the loss of the *pomca* in a *cyp17a1*-deficient background to reduce the testosterone levels. As a result, increased body lipid content with no enhanced body weight gain was observed in these double mutant fish (Figure 6B and D). These data indicated that hyperandrogenism is necessary for the absence of obesity observed in our *pomca* M1 fish model, whereas obesity was observed in all mammalian *pomc*-deficient models.

qRT-PCR for *pomca* mRNA relative expression in M2 and M3 zebrafish brain and pituitary gland were performed at the adult stage (5 mpf). In M2 zebrafish, *pomca* mRNA relative expression level was increased by 22-fold compared with WT fish (Supplementary Figure S6A). In M3 zebrafish, *pomca* mRNA relative expression level was decreased significantly (Supplementary Figure S6A). The cortisol levels in *pomca* M3 zebrafish at the larvae stage were unchanged (Table 2), but it was significantly decreased by 35% at 5 mpf (Supplementary Figure S6B). The decreased cortisol levels in M3 fish were much lower than those in M1 zebrafish by 85.33% (Table 1). However, no phenotypes in terms of body weight and moving distance were observed in M3 zebrafish compared with WT fish at 5 mpf stage (Table 2; Supplementary Figure S6C). Testosterone levels were also measured, and no difference was observed in M3 fish (Table 2). Therefore, it seems like that the significant decreased levels of cortisol could not be sufficient to promote somatic growth in M3 fish. These results also strengthen the conclusion that hyperandrogenism was essential for increased somatic growth in M1 zebrafish. Moreover, we injected M2 or M3 *pomca* mRNA into M1 zebrafish embryo at 1-cell or 2-cell stage. The early phenotype of the disrupted dark-induced melanosome dispersal was used for assessment of rescue effects in the M2 or M3 mRNA overexpression. It has been observed that the partially rescued effects seen (5 out of 10) only in M2 *pomca* mRNA injected zebrafish at 4 dpf (Supplementary Figure S6D–E). The cause of this result may be due to the regulated effects of the melanosome dispersal by β-MSH rather than α-MSH in early zebrafish stages, since intact region of β-MSH presence in M2 mRNA.

The primary features of PCOS are hyperandrogenism, polycystic ovaries, and anovulation. It is also associated with obesity and insulin resistance. The search for PCOS susceptibility genes has mainly focused on genes involved in pathways regulating metabolism, synthesis of sex hormone and regulators, insulin sensitivity, and body weight. Genome-wide association study (GWAS) has identified PCOS candidate loci including

cyp11a1, *cyp17a1*, *ar*, *mc4r*, *pparg*, and *pomc* (Pau et al., 2013). The core diagnostic criteria for PCOS are quite similar to those of another common endocrine disorder, nonclassic congenital adrenal hyperplasia (NCAH)/21-hydroxylase (*cyp21*) deficiency. The defective CYP21 in NCAH leads to cortisol deficiency. The reduced cortisol production then stimulates ACTH levels, which causes adrenocortical growth and eventual adrenal hyperplasia. Furthermore, accumulated of cortisol precursors due to the CYP21 block are shifted to the adrenal and rogen pathway (Speiser et al., 2010). To some extent, the cause of adrenal hyperandrogenism in NCAH is similar to the impaired cortisol synthesis involved in adrenal steroidogenesis process observed in our *pomca*-deficient fish. In addition, a T/C polymorphism in the promoter region of the *cyp17a* gene is associated with PCOS in some cases, which results from the increased activity of *cyp17a* in the rate-limiting steps of androgen biosyn thesis (Diamanti-Kandarakis et al., 1999). There is conflicting evidence regarding the prevalence of obesity in women with PCOS (Ehrmann, 2005). Based on previous reports, the body mass index in PCOS patients related with candidate genes involved in insulin signaling and lipid metabolism (*pparg* and *mc4r*) are tend to be higher than those involved in androgen biosynthesis signaling (*cyp17a* and *cyp21*) (Moran and Azziz, 2003; Antoine et al., 2007; Echiburú et al., 2008; Ewens et al., 2011). This indicates that hyperandrogenism promoted by compensatory hypocortisolism or hyperinsulinemia might be an unappreciated cause of the heterogeneous metabolic status in diagnosed PCOS patients. Because of the difference in *pomc* and leptin signaling in adipostasis between the teleost model and mammals revealed in this study, no hyperinsulinemia or obesity was observed in our *pomca*-deficient fish as observed in *pomc*-null mammals. Therefore, the features of *pomca*-deficient fish would be similar with those observed in NCAH patients and PCOS patients attributed by *cyp17a* polymorphism.

Throughout thousands of years of animal domestication, adrenal hypofunction has been linked to tameness, which leads to a reduction of unnecessary fearful reactivity of livestock animals involved in husbandry (Wilkins et al., 2014). Moreover, it has been reported that the Large White pig breed exhibits a potentially higher production of lean meat with lower HPA axis activity compared with the Meishan breed (Terenina et al., 2013). Some strains of fish used for aquaculture are currently undergoing domestication around the world. High plasma cortisol levels have been reported to be associated with certain growth-stunted farmed Atlantic salmon strains (Vindas et al., 2016). In the present study, a deficiency in the HPI axis resulted in a combined phenotype of enhanced somatic growth and reduced anxiety-related behavioral responses. These findings show that certain polymorphisms of genes involved in the HPI signal cascade, such as *crhr*, *pomc*, *mc2r*, and *hsd3β1*, might be used as new potential breeding markers for the identification of genomic variants during the course of genetic breeding of cultured fish, by improving domesticates for both the traits of tameness and high FCE simultaneously.

Materials and methods

Measurement of plasma cAMP and testosterone concentration

For plasma collection, adult zebrafish were anesthetized in 0.02% MS-222. The tail aorta was severed with scissors, and whole blood was collected from the wound with heparin-treated tips. The plasma was isolated by centrifugation at 4°C and 1500× *g* for 15 min and was stored at −80°C for later analysis. The cAMP and testosterone levels in the zebrafish plasma were measured using the cyclic AMP EIA Kit (Item No. 581001) and testosterone EIA kit (Item No. 582701), respectively, which were purchased from Cayman Chemical Company, following the procedures provided by the manufacturer.

Cortisol content measurement

In view of the circadian rhythms, zebrafish were anesthetized with MS-222 at 9:00 am. For 6 dpf larval zebrafish, a pool of 30 larvae were homogenized in 500 µl cold PBS and then homogenized. At least eight 30-fish pools of each genotype were measured. Plasma was collected from 150 dpf zebrafish. The cortisol content was measured with a cortisol express EIA kit (Item No. 500370) from Cayman Chemical Company following the procedure provided by the manufacturer.

[1-^{14}C] palmitate oxidation in muscle tissue homogenates

[1-^{14}C] palmitate β-oxidation was performed as previously reported (Ning et al., 2017). The muscle tissue was collected from *pomca* mutant 1 and control siblings at 150 dpf. Palmitic acid [1-^{14}C] (PerkinElmer, NEC075H250UC) was used. The radioactivity was determined using a Tri-Carb 4910TR Liquid Scintillation Analyzer (PerkinElmer).

Catabolic rate assays in live fish

Catabolic assays of the intraperitoneally injected L-[^{14}C(U)] amino acid mixture (PerkinElmer, NEC999E000MC) and D-[1-^{14}C] glucose (PerkinElmer, NEC043X250UC) in living fish were performed as previously described (Ning et al., 2017). The KOH solution containing [1-^{14}C] carbon dioxide sourced from the breakdown of the [1-^{14}C] amino acid mixture and D-[1-^{14}C] glucose was collected after 2 h. The muscle tissue samples were also collected and digested with $HClO_4/H_2O_2$ (2:1) at 60°C. The radioactivity of KOH and muscle tissue samples was determined using Tri-Carb 4910TR Liquid Scintillation Analyzer (PerkinElmer).

Quantification and statistical analysis

Differences between the two groups were compared using Student's *t*-test in Statistical Package for the Social Sciences (SPSS version 19.0). The data are represented as the means ± standard deviation (SD) and a probability of $P < 0.05$ was considered to be significant. All the figures were created by Prism (GraphPad Prism, Prism 6.0).

Supplementary material

Supplementary material is available at *Journal of Molecular Cell Biology* online.

Acknowledgements

We are grateful to Xi Li (Institute of Mental Health, Kangning Hospital, Wenzhou, China) for assistance with the zebrafish behavioral assays and helpful comments.

Funding

This work was supported by the National Key R&D Program of China (2018YFD0900404 to J.He and 2018YFD0900205 to Z.Y.), the National Natural Science Foundation of China (31530077 to Z.Y.), and the Pilot Program A Project from the Chinese Academy of Sciences (XDA08010405 to Z.Y.).

Conflict of interest: none declared.

References

Alsop, D., Ings, J.S., and Vijayan, M.M. (2009). Adrenocorticotropic hormone suppresses gonadotropin-stimulated estradiol release from zebrafish ovarian follicles. PLoS One *4*, e6463.

Anderson, E.J., Cakir, I., Carrington, S.J., et al. (2016). 60 years of POMC: regulation of feeding and energy homeostasis by α-MSH. J. Mol. Endocrinol. *56*, T157–T174.

Antoine, H.J., Pall, M., Trader, B.C., et al. (2007). Genetic variants in peroxisome proliferator-activated receptor gamma influence insulin resistance and testosterone levels in normal women, but not those with polycystic ovary syndrome. Fertil. Steril. *87*, 862–869.

Coll, A.P., Challis, B.G., López, M., et al. (2005). Proopiomelanocortin-deficient mice are hypersensitive to the adverse metabolic effects of glucocorticoids. Diabetes *54*, 2269–2276.

Diamanti-Kandarakis, E., Bartzis, M.I., Zapanti, E.D., et al. (1999). Polymorphism T→C (−34 bp) of gene CYP17 promoter in Greek patients with polycystic ovary syndrome. Fertil. Steril. *71*, 431–435.

Dores, R.M., Londraville, R.L., Prokop, J., et al. (2014). Molecular evolution of GPCRs: melanocortin/melanocortin receptors. J. Mol. Endocrinol. *52*, T29–T42.

Dunaif, A., Segal, K.R., Futterweit, W., et al. (1989). Profound peripheral insulin resistance, independent of obesity, in polycystic ovary syndrome. Diabetes *38*, 1165–1174.

Echiburú, B., Pérez-Bravo, F., Maliqueo, M., et al. (2008). Polymorphism T→C (−34 base pairs) of gene CYP17 promoter in women with polycystic ovary syndrome is associated with increased body weight and insulin resistance: a preliminary study. Metabolism *57*, 1765–1771.

Ehrmann, D.A. (2005). Polycystic ovary syndrome. New Engl. J. Med. *352*, 1223–1236.

Ewens, K.G., Jones, M.R., Ankener, W., et al. (2011). FTO and MC4R gene variants are associated with obesity in polycystic ovary syndrome. PLoS One *6*, e16390.

Ewens, K.G., Stewart, D.R., Ankener, W., et al. (2010). Family-based analysis of candidate genes for polycystic ovary syndrome. J. Clin. Endocrinol. Metab. *95*, 2306–2315.

Fei, F., Sun, S., Yao, Y., et al. (2017). Generation and phenotype analysis of zebrafish mutations of obesity-related genes lepr and mc4r. Sheng Li Xue Bao *69*, 61–69.

Gallo-Payet, N. (2016). 60 years of POMC: adrenal and extra-adrenal functions of ACTH. J. Mol. Endocrinol. *56*, T135–T156.

Gao, Y., Dai, Z., Shi, C., et al. (2016). Depletion of myostatin b promotes somatic growth and lipid metabolism in zebrafish. Front. Endocrinol. *7*, 88.

Gonzalez-Nunez, V., Gonzalez-Sarmiento, R., and Rodríguez, R.E. (2003). Identification of two proopiomelanocortin genes in zebrafish (Danio rerio). Brain Res. Mol. Brain Res. *120*, 1–8.

Hansen, I.A., To, T.T., Wortmann, S., et al. (2003). The pro-opiomelanocortin gene of the zebrafish (Danio rerio). Biochem. Biophys. Res. Commun. *303*, 1121–1128.

Huszar, D., Lynch, C.A., Fairchild-Huntress, V., et al. (1997). Targeted disruption of the melanocortin-4 receptor results in obesity in mice. Cell *88*, 131–141.

Kadi, F. (2008). Cellular and molecular mechanisms responsible for the action of testosterone on human skeletal muscle. A basis for illegal performance enhancement. Br. J. Pharmacol. *154*, 522–528.

Kelly, D., and Jones, T. (2015). Testosterone and obesity. Obes. Rev. *16*, 581–606.

Krude, H., Biebermann, H., Luck, W., et al. (1998). Severe early-onset obesity, adrenal insufficiency and red hair pigmentation caused by POMC mutations in humans. Nat. Genet. *19*, 155–157.

Lee, Y.S., Challis, B.G., Thompson, D.A., et al. (2006). A POMC variant implicates β-melanocyte-stimulating hormone in the control of human energy balance. Cell Metab. *3*, 135–140.

Li, D., Lou, Q., Zhai, G., et al. (2014). Hyperplasia and cellularity changes in IGF-1-overexpressing skeletal muscle of crucian carp. Endocrinology *155*, 2199–2212.

Lin, J.-C., Hu, S., Ho, P.-H., et al. (2015). Two zebrafish hsd3b genes are distinct in function, expression, and evolution. Endocrinology *156*, 2854–2862.

Martin, R., Savage, D., Carson, D., et al. (2011). Association analysis of proopiomelanocortin (POMC) haplotypes in type 1 diabetes in a UK population. Diabetes Metab. *37*, 298–304.

Michel, M., Page-McCaw, P.S., Chen, W., et al. (2016). Leptin signaling regulates glucose homeostasis, but not adipostasis, in the zebrafish. Proc. Natl Acad. Sci. USA *113*, 3084–3089.

Moran, C., and Azziz, R. (2003). 21-hydroxylase-deficient nonclassic adrenal hyperplasia: the great pretender. Semin. Reprod. Med. *21*, 295–300.

Ning, L.-J., He, A.-Y., Lu, D.-L., et al. (2017). Nutritional background changes the hypolipidemic effects of fenofibrate in Nile tilapia (Oreochromis niloticus). Sci. Rep. *7*, 41706.

Notake, M., Tobimatsu, T., Watanabe, Y., et al. (1983). Isolation and characterization of the mouse corticotropin-β-lipotropin precursor gene and a related pseudogene. FEBS Lett. *156*, 67–71.

Pau, C., Saxena, R., and Welt, C.K. (2013). Evaluating reported candidate gene associations with polycystic ovary syndrome. Fertil. Steril. *99*, 1774–1778.

Peng, X., Lin, J., Zhu, Y., et al. (2016). Anxiety-related behavioral responses of pentylenetetrazole-treated zebrafish larvae to light–dark transitions. Pharmacol. Biochem. Behav. *145*, 55–65.

Raffan, E., Dennis, R.J., O'Donovan, C.J., et al. (2016). A deletion in the canine POMC gene is associated with weight and appetite in obesity-prone Labrador retriever dogs. Cell Metab. *23*, 893–900.

Rainey, W.E., and Nakamura, Y. (2008). Regulation of the adrenal androgen biosynthesis. J. Steroid Biochem. Mol. Biol. *108*, 281–286.

Rosa, C.E., Figueiredo, M.A., Lanes, C.F.C., et al. (2008). Metabolic rate and reactive oxygen species production in different genotypes of GH-transgenic zebrafish. Comp. Biochem. Physiol. B Biochem. Mol. Biol. *149*, 209–214.

Rossetti, M.L., Steiner, J.L., and Gordon, B.S. (2017). Androgen-mediated regulation of skeletal muscle protein balance. Mol. Cell. Endocrinol. *447*, 35–44.

Rubinstein, M., Mogil, J.S., Japón, M., et al. (1996). Absence of opioid stress-induced analgesia in mice lacking β-endorphin by site-directed mutagenesis. Proc. Natl Acad. Sci. USA *93*, 3995–4000.

Schwartz, M.W., Woods, S.C., Porte, D., Jr, et al. (2000). Central nervous system control of food intake. Nature *404*, 661–671.

Speiser, P.W., Azziz, R., Baskin, L.S., et al. (2010). Congenital adrenal hyperplasia due to steroid 21-hydroxylase deficiency: an Endocrine Society clinical practice guideline. J. Clin. Endocrinol. Metab. *95*, 4133–4160.

Terenina, E., Babigumira, B.M., Le, G., et al. (2013). Association study of molecular polymorphisms in candidate genes related to stress responses with production and meat quality traits in pigs. Domest. Anim. Endocrinol. *44*, 81–97.

To, T.T., Hahner, S., Nica, G., et al. (2007). Pituitary–interrenal interaction in zebrafish interrenal organ development. Mol. Endocrinol. *21*, 472–485.

Tokarz, J., Möller, G., de Angelis, M.H., et al. (2013). Zebrafish and steroids: what do we know and what do we need to know? J. Steroid Biochem. Mol. Biol. *137*, 165–173.

Uhler, M., Herbert, E., d'Eustachio, P., et al. (1983). The mouse genome contains two nonallelic pro-opiomelanocortin genes. J. Biol. Chem. *258*, 9444–9453.

Urbanek, M., Legro, R.S., Driscoll, D.A., et al. (1999). Thirty-seven candidate genes for polycystic ovary syndrome: strongest evidence for linkage is with follistatin. Proc. Natl Acad. Sci. USA *96*, 8573–8578.

Usui, T., Kajita, K., Kajita, T., et al. (2014). Elevated mitochondrial biogenesis in skeletal muscle is associated with testosterone-induced body weight loss in male mice. FEBS Lett. *588*, 1935–1941.

Vindas, M.A., Johansen, I.B., Folkedal, O., et al. (2016). Brain serotonergic activation in growth-stunted farmed salmon: adaption versus pathology. R. Soc. Open Sci. *3*, 160030.

Wagle, M., Mathur, P., and Guo, S. (2011). Corticotropin-releasing factor critical for zebrafish camouflage behavior is regulated by light and sensitive to ethanol. J. Neurosci. *31*, 214–224.

Wilkins, A.S., Wrangham, R.W., and Fitch, W.T. (2014). The 'domestication syndrome' in mammals: a unified explanation based on neural crest cell behavior and genetics. Genetics *197*, 795–808.

Yaswen, L., Diehl, N., Brennan, M.B., et al. (1999). Obesity in the mouse model of pro-opiomelanocortin deficiency responds to peripheral melanocortin. Nat. Med. *5*, 1066–1070.

Zhai, G., Shu, T., Xia, Y., et al. (2017). Androgen signaling regulates the transcription of anti-Müllerian hormone via synergy with SRY-related protein SOX9A. Sci. Bull. *62*, 197–203.

Zhang, C., Forlano, P.M., and Cone, R.D. (2012). AgRP and POMC neurons are hypophysiotropic and coordinately regulate multiple endocrine axes in a larval teleost. Cell Metab. *15*, 256–264.